Molecular Docking Studies and Synthesis of Amino-oxy-diarylquinoline Derivatives as Potent Non-nucleoside HIV-1 Reverse Transcriptase Inhibitors

Authors

Arthit Makarasen[1], Mayuso Kuno[3], Suwicha Patnin[3], Nanthawan Reukngam[1], Panita Khlaychan[1], Sirinya Deeyohe[1], Pakamas Intachote[2], Busakorn Saimanee[2], Suchada Sengsai[2], Pornthip Boonsri[3], Apinya Chaivisuthangkura[3], Wandee Sirithana[4], Supanna Techasakul[1]

Affiliations

1 Department of Chemistry, Laboratory of Organic Synthesis, Chulabhorn Research Institute, Laksi, Bangkok, Thailand
2 Biological Activity Test and Screening Unit, Central Facilities, Chulabhorn Research Institute, Laksi, Bangkok, Thailand
3 Department of Chemistry, Faculty of Science, Srinakharinwirot University, Wattana, Bangkok, Thailand
4 Department of Chemical Technology, Faculty of Science and Technology, Suan Dusit University, Bangplat, Bangkok

Keywords

synthesis, quinoline, molecular docking, hybrid, anti HIV-1 activity

received 08.03.2019
accepted 02.07.2019

Bibliography

DOI https://doi.org/10.1055/a-0968-1150
Published online: 7.11.2019
Drug Res 2019; 69: 671–682

ISSN 2194-9379

Correspondence

Dr. Supanna Techasakul
Department of Chemistry
Laboratory of Organic Synthesis, Chulabhorn Research Institute
Laksi
10210 Bangkok
Thailand
Tel.: + 66/255/38 555, Fax: + 66/255/38 549
supanna@cri.or.th

Supporting Information for this article is available online at http://www.thieme-connect.de/products.

ABSTRACT

In this study, amino-oxy-diarylquinolines were designed using structure-guided molecular hybridization strategy and fusing of the pharmacophore templates of nevirapine (NVP), efavirenz (EFV), etravirine (ETV, TMC125) and rilpivirine (RPV, TMC278). The anti-HIV-1 reverse transcriptase (RT) activity was evaluated using standard ELISA method, and the cytotoxic activity was performed using MTT and XTT assays. The primary bioassay results indicated that 2-amino-4-oxy-diarylquinolines possess moderate inhibitory properties against HIV-1 RT. Molecular docking results showed that 2-amino-4-oxy-diarylquinolines **8(a-d)** interacted with the Lys101 and His235 residue though hydrogen bonding and interacted with Tyr318 residue though π-π stacking in HIV-1 RT. Furthermore, **8a** and **8d** were the most potent anti-HIV agents among the designed and synthesized compounds, and their inhibition rates were 34.0 % and 39.7 % at 1 µM concentration. Interestingly, **8a** was highly cytotoxicity against MOLT-3 (acute lymphoblastic leukemia), with an IC_{50} of 4.63 ± 0.62 µg/mL, which was similar with that in EFV and TMC278 (IC_{50} 7.76 ± 0.37 and 1.57 ± 0.20 µg/ml, respectively). Therefore, these analogs of the synthesized compounds can serve as excellent bases for the development of new anti-HIV-1 agents in the near future.

Introduction

Acquired immune deficiency syndrome (AIDS) is caused by human immunodeficiency virus (HIV). The research on this disease has been extensive for over 40 years, but no cure has been found. Multi-drug therapy against HIV, known as highly active antiretroviral therapy (HAART), has become the most standard and efficient treatment regimen for HIV infection. HAART generally involves inhibitors targeting reverse transcriptase (RT) and protease enzymes [1–3]. Among the currently available drugs in HAART, RT inhibitors are the mainstay of most of the frontline HIV combination therapies. The RT inhibitors can be divided into two classes of drugs, namely, those belonging to the nucleoside reverse transcriptase (NRTIs) and those belonging to the non- nucleoside reverse transcriptase (NNRTIs) [4]. NRTIs inhibit the RT through the active site, whereas the NNRTIs bind to a site far from the active site [5–7]. NNRTIs are important components of the HAART regimen, owing to their unique antiviral activity, high specificity and low cytotoxicity. The five structurally diverse NNRTIs, namely, nevirapine (NVP), delavirdine (DLV), efavirenz (EFV) [8, 9], etravirine (ETV, TMC125) and rilpivirine (RPV, TMC278) [10, 11], were approved by FDA for clinical use. Searching for new anti-HIV-1 RT agent with either higher potency or less toxicity is necessary, and researchers focus on finding solution to this problem. Molecular hybridization approach is used to design and develop new molecules. This approach depends on the combination of physiochemical and pharmacological activities to produce newly hybridized compounds with improved affinity and efficiency compared with drugs containing two or more known compounds. In the present study, we studied the molecular hybridization of NVP, EFV, and TMC278 to generate a series of disubstituted quinoline derivatives and to explore the new anti-HIV agents.

Quinoline is a heterocyclic aromatic nitrogen compound widely used as a parental compound to synthesize molecules with medical benefits. Quinoline derivatives are an important class of heterocycles, being the chief components of many naturally occurring products. The quinoline derivative possesses various pharmacological properties, such as anticancer, antimycobacterial, antimicrobial, anticonvulsant, anti-inflammatory and cardiovascular activities [12–16]. The applications of quinoline derivatives utilizes in almost every branch of medicinal chemistry. In recent years, large numbers of quinoline derivatives, including mono-, di-, tri-, tetra- and heterocyclic substituents have been synthesized and their cytotoxic activity reported [17]. Our research program aimed at the discovery of HIV-1 RT using the quinoline as a core structure to maintain the characteristic of the original base structure. The molecular hybridizations are characterized by a core structure of quinoline and the substituent for two positions in the core structure. Similar side chains of TMC125 and TMC278 were used to confirm the potential of this core structure in the NNRTI activity. Herein, we reported the synthesis and antiviral activity of amino-oxydiarylquinoline derivatives together with some measured and calculated physicochemical properties, such as binding energy, number of ligand conformations and interaction. The possible structures and the structure-activity relationships are discussed in detail to obtain further insights into these analogs.

Material and Methods

The starting materials and other reagents for synthesis were purchased from Aldrich Company and Tokyo Chemical Industry and were used as received without further purification unless otherwise indicated. The melting points were measured using an SMP3 Stuart™ digital melting point apparatus from Bibby Sterlin, Ltd. To confirm the structure, we analyzed the product by using nuclear magnetic resonance (NMR) and mass spectrometry. Proton and carbon NMR spectra were obtained using the Bruker AvanceII-300 spectrometer at 300 and 75 MHz, respectively. High-resolution mass spectra were measured with an ESI-TOF, i. e., MicroTOF mass spectrometer (Bruker Daltonics, Germany). HepG2(hepatocarcinoma), MOLT-3 (acute lymphoblastic leukemia), HuCCA-1 (cholangiocarcinoma), A549 (lung carcinoma), and MRC-5 (normal embryonic lung cell) cell lines were purchased from Hyclone Laboratories. Doxorubicin (purity ≥ 98 %) and etoposide (purity 98 %) were purchased from Aldrich Company.

Molecular docking studies

The geometry of quinoline derivatives, namely, **5(a-d)** and **8(a-d)** was fully optimized using the density functional theory (DFT) at B3LYP/6–31 G (d, p) level implemented in Gaussian 03. The crystal structure of HIV-1(4G1Q) was obtained from the Protein Data Bank. 4G1Q is a crystal structure of HIV-1 RT in a complex with TMC278, which is an NNRTI. Before docking, the protein was prepared by removing water molecules, the ligand, and other unnecessary small molecules from the crystal structure of the ligand-HIV-1 RT complex (PDB code: 4G1Q). The binding interactions of quinoline derivatives with HIV-1 were simulated by molecular docking using the Autodock 4.2. Autodock default settings were used for parameters such as the population size for the Lamarckian Genetic Algorithm (LGA) (set to 150 individuals) and the number of genetic algorithm (set to 200). The maximum number of evaluations was performed for 2 500 000 and the maximum number of generations was selected for 27 000. The grid box size used was 80 × 80 × 80 A° and the center applied was as follows: x = 49.082, y = − 28.29, z = 37.541; the spacing was 0.375 A°. The lowest energy conformation was used to visualize the docked conformation using the Discovery studio 4.0 software. The identification of ligand binding modes was done by iteratively evaluating a number of ligand conformations and estimating energy of their interactions with the target. Experiment were performed in triplicate and repeated three times with similar results.

Synthesis

6-Nitroquinolin-4-ol **(2)**

A mixture of concentrated nitric acid (2.5 mL) and concentrated sulfuric acid (2.5 mL) was slowly added to a solution of 4-hydroxyquinoline (**1)** (2.0 g, 13.8 mmol) in concentrated sulfuric acid (2.5 mL) at − 15 °C. The mixture was stirred for 2 h, and the temperature of the reaction mixture was slowly raised from − 15 to 0 °C. The mixture was quenched with ice-water (1:1). The precipitated crude product, that is, **2**, was collected by filtration and dried under high vacuum (2.2 g, 84 %), yellow solid, and mp. 217.5 °C–218.4 °C. The ^{1}H-NMR (300 MHz, dimethyl sulfoxide-d6 [DMSO-d6]) conditions were as follows: δ ppm 6.20 (d, 1 H, J = 7.5 Hz), 7.73 (d, 1 H,

J = 9.1 Hz), 8.06 (d, 1 H, J = 7.5 Hz), 8.42 (dd, 1 H, J = 9.2, 2.7 Hz), 8.84 (d, 1 H, J = 2.7 Hz), and 12.33 (bs, 1 H). The ^{13}C-NMR (75 MHz, DMSO-d6) conditions were as follows: δ ppm 110.2, 110.5, 120.2, 121.6, 124.6, 125.9, 140.9, 142.6, 143.7, and 176.3. Finally, the HRMS (+ ESI) was $C_9H_7N_2O_3$ $[M+H]^+$; it requires 191.0457, but has 191.0448.

4-Chloro-6-nitroquinoline **(3)**

A catalytic amount of DMF was added to the mixture of **2** (1.0 g, 5.3 mmol) and $POCl_3$ (20 mL) in a sealed tube. The sealed tube was flushed with argon, and the reaction mixture was heated at 100 °C for 5 h. The excess of $POCl_3$ was removed from the reaction mixture under high vacuum. Furthermore, 10 % aqueous NH_4OH was added to the residue and extracted thrice with ethyl acetate. The combined organic layers were washed with saturated NaCl and dried over Na_2SO_4. The crude product was purified on silica gel column (eluent: hexane/ethyl acetate 1:1) to obtain **3** (1.0 g, 91 %), white solid and mp. 140.8 °C–141.5 °C. The ^{1}H-NMR (300 MHz, $CDCl_3$) conditions were as follows: δ ppm 7.67 (d, 1 H, J = 3.5 Hz), 8.23 (d, 1 H, J = 6.9 Hz), 8.55 (dd, 1 H, J = 6.9, 1.2 Hz), 8.97 (dd, 1 H, J = 3.5 Hz), and 9.20 (bs, 1 H). The ^{13}C-NMR (75 MHz, $CDCl_3$) conditions were as follows: δ ppm 121.4, 122.9, 123.9, 125.9, 132.0, 144.6, 151.0, and 153.3. Finally, the HRMS (+ ESI) was $C_9H_6ClN_2O_2$ $[M+H]^+$; it requires 209.0118, but has 209.0112.

General procedure for the preparation of 4-phenoxy-6-nitroquinoline 4(a-d)

A mixture of **3** (0.48 mmol) and hydroxyl benzene (0.57 mmol) in DMF (4 mL) with anhydrous potassium carbonate (0.96 mmol) was heated in a sealed tube and stirred at 120 °C for 5 h. After cooling, the mixture was poured into ice-water, and the mixture was extracted thrice with ethyl acetate. The combined organic layers were washed with saturated NaCl and dried over Na_2SO_4. The crude product was purified on silica gel column (eluent: hexane/ethyl acetate) to obtain 4-phenoxy-6-nitroquinoline **4(a-d)**

4-(2′,6′-Dimethyl-4′-formylphenoxy)-6-nitroquinoline **(4a)**

With 97 % yield, the synthesis started with 100 mg (0.48 mmol) of **3** to obtain 150 mg of **4a**, which consisted of white solid, and mp. 183.0 °C–183.7 °C. The ^{1}H-NMR (300 MHz, $CDCl_3$) conditions were as follows: δ ppm 2.25 (s, 6 H), 6.41 (d, 1 H, J = 5.2 Hz), 7.77 (s, 2 H), 8.27 (d, 1 H, J = 9.3 Hz), 8.56 (dd, 1 H, J = 9.3, 2.3 Hz), 8.82 (d, 1 H, J = 5.2 Hz), 9.42 (d, 1 H, J = 2.5 Hz), and 10.03 (s, 1 H). The ^{13}C-NMR (75 MHz, $CDCl_3$) conditions were as follows: δ ppm 103.4, 119.1, 119.6, 123.8, 130.8, 131.0, 131.1, 132.0, 134.5, 145.4, 151.7, 154.2, 154.7, and 160.9. Finally, the HRMS (+ ESI) was $C_{18}H_{15}N_2O_4$ $[M+H]^+$; it requires 323.1032, but has 323.1024.

4-(2′,6′-Dimethyl-4′-cyanophenoxy)-6-nitroquinoline **(4b)**

With 90 % yield, the synthesis started with 100 mg (0.48 mmol) of **3** to obtain 138 mg of **4b**, which consisted of white solid, and mp. 226.0 °C–226.7 °C. The ^{1}H-NMR (300 MHz, $CDCl_3$) conditions were as follows: δ ppm 2.20 (s, 6 H), 6.36 (d, 1 H, J = 3.9 Hz), 7.55 (s, 2 H), 8.27 (d, 1 H, J = 7.0 Hz), 8.57 (dd, 1 H, J = 7.0, 1.7 Hz), 8.82 (d, 1 H, J = 3.9 Hz), and 8.39 (d, 1 H, J = 1.8 Hz). The ^{13}C-NMR (75 MHz, $CDCl_3$) conditions were as follows: δ ppm 16.0, 103.2, 110.7, 118.1, 119.0, 119.5, 123.9, 131.2, 132.7, 133.3, 145.5, 151.8, 153.0, 154.7, and 160.7. Finally, the HRMS (+ ESI) was $C_{18}H_{14}N_3O_3$ $[M+H]^+$; it requires 320.1035, but has 320.1020.

4-(4′-formylphenoxy)-6-nitroquinoline **(4c)**

With 90 % yield, the synthesis started with 100 mg (0.48 mmol) of **3** to obtain 127 mg of **4c**, which consisted of white solid and mp. 203.8 °C–204.3 °C. The ^{1}H-NMR (300 MHz, $CDCl_3$) conditions were as follows: δ ppm 6.78 (d, 1 H, J = 5.2 Hz), 7.40 (dd, 2 H, J = 6.8, 1.7 Hz), 8.06 (dt, 2 H, J = 8.6, 1.9 Hz), 8.26 (d, 1 H, J = 9.3 Hz), 8.55 (dd, 1 H, J = 9.3, 2.6 Hz), 8.90 (d, 1 H, J = 5.2 Hz), 9.30 (d, 1 H, J = 2.5 Hz), and 10.07 (s, 1 H). The ^{13}C-NMR (75 MHz, $CDCl_3$) conditions were as follows: δ ppm 106.1, 119.3, 120.6, 121.3, 123.9, 131.2, 132.3, 134.3, 151.8, 154.6, 158.5, 162.0, and 190.4. Finally, the HRMS (+ ESI) was $C_{16}H_{10}N_2O_4$ $[M+H]^+$; it requires 294.0641, but has 295.0714.

4-(4′-cyanophenoxy)-6-nitroquinoline **(4d)**

With 99 % yield, the synthesis started with 100 mg (0.48 mmol) of **3** to obtain 138 mg of **4d**, which consisted of white solid, mp. 212.4 °C–213.3 °C. The ^{1}H-NMR (300 MHz, $CDCl_3$) conditions were as follows: δ ppm 6.77 (d, 1 H, J = 3.9 Hz), 7.36 (d, 2 H, J = 6.5 Hz), 7.84 (d, 2 H, J = 6.45 Hz), 8.26 (d, 1 H, J = 6.7 Hz), 8.55 (dd, 1 H, J = 6.9, 1.8 Hz), 8.91 (d, 1 H, J = 3.8 Hz), and 9.27 (d, 1 H, J = 1.9 Hz). The ^{13}C-NMR (75 MHz, $CDCl_3$) conditions were as follows: δ ppm 106.1, 110.2, 117.8, 119.1, 120.5, 121.7, 124.0, 131.3, 134.8, 145.6, 151.8, 154.5, 157.2, and 161.7. Finally, the HRMS (+ ESI) was $C_{16}H_{10}N_3O_3$ $[M+H]^+$; it requires 292.0722, but has 292.0709.

General procedure for the preparation of 4-oxyaryl-6-(4'-cyanophenyl)-aminoquinoline 5(a-d)

A mixture of **4(a-d)** (0.10 mmol) and $SnCl_2 \cdot 2H_2O$ (0.50 mmol) in absolute ethanol (3 mL) was sonicated in a water bath at 30 °C for 2 h. When the whole starting material was completely consumed in the reaction (identified by the TLC), the mixture was cooled to room temperature and the solvent was evaporated. The residue was dissolved with ethyl acetate and filtered through a short silica gel column. The crude product was used for further reaction without purification. A mixture of 6-(4-phenoxy)-quinolinamine (0.10 mmol), 4-iodobenzonitrile (0.12 mmol), $Pd(OAc)_2$ (0.01 mmol), SPhos (0.01 mmol) and Cs_2CO_3 (0.15 mmol) in DMF (5 mL) was stirred and heated at 100 °C for 10 h. After cooling, the corresponding solution was evaporated in vacuo. The residue was purified on silica gel column (eluent: hexane/ethyl acetate) to obtain **5(a-d)**.

4-(2′,6′-Dimethyl-4′-formylphenoxy)-6-(4′′-cyanophenyl)-aminoquinoline **(5a)**

With 38 % yield (2 steps), the synthesis started with 32.4 mg (0.10 mmol) of **4a** to obtain 15.2 mg of **5a**, which consisted of yellow solid and mp. 276.5 °C–277.2 °C. **5a** was obtained in 28.2 % overall yield (5 steps from **1**). The ^{1}H-NMR (300 MHz, $CDCl_3$) conditions were as follows: δ ppm 2.22 (s, 6 H), 6.24 (d, 1 H, J = 5.2 Hz), 6.57 (s, 1 H), 7.15–7.22 (m, 2 H), 7.54–7.60 (m, 2 H), 7.64 (dd, 1 H, J = 8.0, 2.6 Hz), 7.73 (s, 2 H), 8.10–8.18 (m, 2 H), 8.55 (d, 1 H, J = 5.2 Hz), and 10.00 (s, 1 H). The ^{13}C-NMR (75 MHz, $CDCl_3$) conditions were as follows: δ ppm 14.1, 14.1, 102.6, 109.0, 115.9, 121.4, 125.2, 130.4, 130.9, 132.2, 133.9, 134.3, 138.8, 146.9, 149.3,

154.9, 159.0, and 191.2. Finally, the HRMS (+ESI) was $C_{25}H_{20}N_3O_2$ $[M+H]^+$; it requires 394.1550, but has 394.1549.

4-(2′,6′-Dimethyl-4′-cyanophenoxy)-6-(4′′-cyanophenyl)-aminoquinoline **(5b)**

With 59 % yield (2 steps), the synthesis started with 20.0 mg (0.06 mmol) of **4b** to obtain 14.5 mg of **5b**, which consisted of yellow solid and mp. 289.5 °C–290.1 °C. **5b** was obtained in 40.6 % overall yield (5 steps from **1**). The ^{1}H-NMR (300 MHz, $CDCl_3$) conditions were as follows: δ ppm 2.15 (s, 6 H), 6.20 (d, 1 H, J = 4.9 Hz), 6.61 (bs, 1 H), 7.18 (d, 2 H, J = 8.7 Hz), 7.56 (bs, 2 H), 7.57 (d, 2 H, J = 2.4 Hz), 7.63 (dd, 1 H, J = 9.0, 2.4 Hz), 8.07–8.15 (m, 2 H), and 8.55 (d, 1 H, J = 5.1 Hz). The ^{13}C-NMR (75 MHz, $CDCl_3$) conditions were as follows: δ ppm 16.0, 102.5, 102.5, 108.9, 110.1, 115.8, 118.3, 119.5, 121.3, 125.1, 130.9, 132.9, 133.2, 133.9, 138.7, 146.7, 147.0, 149.5, 153.7, and 158.5. Finally, the HRMS (+ESI) was $C_{25}H_{19}N_4O$ $[M+H]^+$; it requires 391.1553, but has 391.1550.

4-(4′-formylphenoxy)-6-(4′′-cyanophenyl)-aminoquinoline **(5c)**

With 52 % yield (2 steps), the synthesis started with 20.9 mg (0.07 mmol) of **4c** to obtain 13.4 mg of **5a**, which consisted of yellow solid and mp. 116.0 °C–117.0 °C. **5c** was obtained in 44.2 % overall yield (5 steps from **1**). The ^{1}H-NMR (400 MHz, $CDCl_3$) conditions were as follows: δ ppm 6.40 (bs, 1 H), 6.75 (d, 1 H, J = 5.1 Hz), 7.12 (bd, 2 H, J = 8.8 Hz), 7.29 (bd, 2 H, J = 8.6 Hz), 7.51–7.57 (m, 2 H), 7.59 (dd, 1 H, J = 9.0, 2.6 Hz), 7.91 (d, 1 H, J = 2.5 Hz), 7.96–8.02 (m, 2 H), 8.13 (d, 1 H, J = 9.0 Hz), 8.69 (d, 1 H, J = 5.1 Hz), and 10.0 (s, 1 H). The ^{13}C-NMR (100 MHz, $CDCl_3$) conditions were as follows: δ ppm 103.2, 107.2, 108.7, 115.9, 119.4, 120.3, 122.6, 125.2, 130.9, 132.2, 133.4, 133.9, 138.8, 146.7, 149.4, 159.2, 160.0, and 190.5. Finally, the HRMS (+ESI) was $C_{23}H_{16}N_3O_2$ $[M+H]^+$; it requires 366.1237, but has 366.1232.

4-(4′-cyanophenoxy)-6-(4′′-cyanophenyl)-aminoquinoline **(5d)**

With 63 % yield (2 steps), the synthesis started with 20.9 mg (0.07 mmol) of **4d** to obtain 16.4 mg of **5d**, which consisted of yellow solid and mp. 214.0 °C–214.6 °C. **5d** was obtained in 47.7 % overall yield (5 steps from **1**). The ^{1}H-NMR (300 MHz, $CDCl_3$) conditions were as follows: δ ppm 6.40 (bs, 1 H), 6.73 (d, 1 H, J = 5.0 Hz), 7.11 (bd, 2 H, J = 8.64, 7.24 (bd, 2 H, J = 8.70), 7.50–7.56 (m, 2 H), 7.58 (dd, 1 H, J = 9.2, 2.5 Hz), 7.75 (bd, 2 H, J = 8.7 Hz), 7.87 (d, 1 H, J = 2.4 Hz) , 8.12 (d, 1 H, J = 9 Hz), and 8.69 (d, 1 H, J = 4.98 Hz). The ^{13}C-NMR (75 MHz, $CDCl_3$) conditions were as follows: δ ppm 103.3, 107.3, 108.5, 108.9, 116.0, 118.1, 119.4, 120.6, 122.6, 124.0, 125.2, 131.1, 133.9, 134.6, 138.9, 146.7, 149.4, and 158.7. Finally, the HRMS (+ESI) was $C_{23}H_{15}N_4O$ $[M+H]^+$; it requires 363.1240, but has 363.1246.

General procedure for the preparation of 2-chloro-4-phenoxyquinoline 7(a-d)

A mixture of 2,4-dichloroquinoline (**6**) (5.05 mmol) and hydroxyl benzene (5.56 mmol) in DMF (15 mL) with anhydrous cesium carbonate (10.10 mmol) was heated in a sealed tube and stirred at 80 °C for 16 h. After cooling, the mixture was poured into ice-water, and the mixture was extracted thrice with ethyl acetate. The combined organic layers were washed with saturated NaCl and dried over Na_2SO_4. The crude product was purified on a silica gel column (eluent: hexane/ethyl acetate) to obtain **7(a-d)**.

4-(2′,6′-Dimethyl-4′-formylphenoxy)-2-chloroquinoline **(7a)**

With 69 % yield, the synthesis started with 1.0 g (5.05 mmol) of **6** to obtain 1.1 g of **7a**, which consisted of white solid and mp. 154.6 °C–156.9 °C. The ^{1}H-NMR (300 MHz, $CDCl_3$) conditions were as follows: 2.23 (s, 6 H), 6.20 (s, 1 H), 7.65 (td, 1 H, J = 7.5, 1.2 Hz), 7.75 (s, 2 H), 7.82 (td, 1 H, 7.5, 1.2 Hz), 8.04 (dd, 1 H, 8.3, 0.9 Hz), and 8.4 (dd, 1 H, 8.3, 0.9 Hz). The ^{13}C-NMR (75 MHz, $CDCl_3$) conditions were as follows: 16.1, 102.9, 119.5, 121.7, 126.7, 128.5, 131.5, 132.1, 134.4, 148.8, 151.3, 154.6, 161.0, and 191.2. Finally, the HRMS (+ESI) was $C_{18}H_{15}ClNO_2$ $[M+H]^+$; it requires 312.0791, but has 312.0791.

4-(2′,6′-Dimethyl-4′-cyanophenoxy)-2-chloroquinoline **(7b)**

With 62 % yield, the synthesis started with 0.30 g (1.51 mmol) of **6** to obtain 0.29 g of **7b**, which consisted of white solid and mp. 184.3 °C–185.0 °C. The ^{1}H-NMR (300 MHz, $CDCl_3$) conditions were as follows: 2.20 (s, 6 H), 6.2 (s, 1 H), 7.53 (s, 2 H), 7.65 (td, 1 H, J = 9.2, 1.5 Hz), 7.83 (td, 1 H, J = 9.2, 1.5 Hz), 8.04 (dd, 1 H, J = 8.3, 1.2 Hz), and 8.38 (dd, 1 H, J = 8.3, 1.2 Hz). The ^{13}C-NMR (75 MHz, $CDCl_3$) conditions were as follows: 15.9, 102.7, 110.4, 118.1, 119.3, 121.6, 126.8, 128.4, 131.5, 132.7, 133.3, 148.8, 151.1, 153.2, and 160.7. Finally, the HRMS (+ESI): $C_{18}H_{14}ClN_2O$ $[M+H]^+$; it requires 309.0795, but has 309.0783.

4-(4′-formylphenoxy)-2-chloroquinoline **(7c)**

With 67 % yield, the synthesis started with 0.30 g (1.51 mmol) of **6** to obtain 0.29 g of **7c**, which consisted of white solid and mp. 113.9 °C–114.2 °C. The ^{1}H-NMR (300 MHz, $CDCl_3$) conditions were as follows: 6.64 (s, 1 H), 7.35 (d, 2 H, J = 8.7 Hz), 7.61 (td, 1 H, J = 7.8, 1.2 Hz), 7.81 (td, 1 H, J = 7.8, 1.2 Hz), 8.04 (m, 3 H), and 8.26 (dd, 1 H, J = 8.4, 0.9 Hz). The ^{13}C-NMR (75 MHz, $CDCl_3$) conditions were as follows: 106.5, 120.4, 121.0, 121.8, 126.9, 128.5, 131.6, 132.3, 134.0, 149.0, 151.0, 159.1, 161.9, and 190.5. Finally, the HRMS (+ESI) was $C_{16}H_{11}ClNO_2$ $[M+H]^+$; it requires 284.0478, but has 284.0465.

4-(4′-cyanophenoxy)-2-chloroquinoline **(7d)**

With 60 % yield, the synthesis started with 0.30 g (1.51 mmol) of **6** to obtain 0.26 mg of **7d**, which consisted of white solid and mp. 214.1 °C–215.0 °C. The ^{1}H-NMR (300 MHz, $CDCl_3$) conditions were as follows: 6.63 (s, 1 H), 7.32 (d, 2 H), 7.60 (t, 1 H, J = 7.2 Hz), 7.78–7.83 (m, 3 H), 8.02 (d, 1 H, J = 8.4 Hz), and 8.22 (d, 1 H, J = 8.4 Hz). The ^{13}C-NMR (75 MHz, $CDCl_3$) conditions were as follows: 106.4, 109.6, 117.9, 119.6, 120.2, 121.2, 121.6, 126.9, 128.4, 131.5, 134.4, 134.7, 148.8, 150.8, 157.6, 161.5. Finally, the HRMS (+ESI) was $C_{16}H_{10}ClN_2O$ $[M+H]^+$; it requires 281.0482, but has 281.0470

General procedure for the preparation of 2-amino-4-oxydiarylquinoline 8(a-d)

A mixture of 2-chloro-4-phenoxyquinoline **7(a-d)** (0.13 mmol), 4-iodobenzonitrile (0.17 mmol), $Pd(OAc)_2$ (0.01 mmol), SPhos (0.01 mmol) and Cs_2CO_3 (0.20 mmol) in DMF (7 mL) was stirred and

heated at 100 °C for 5 h. After cooling, the corresponding solution was evaporated in vacuo. The residue was purified on a silica gel column (eluent: hexane/ethyl acetate) to obtain **8(a-d)**.

4-(2′,6′-Dimethyl-4′-formylphenoxy)-2-(4′′-cyanophenyl)-aminoquinoline **(8a)**

With 69 % yield, the synthesis started with 40.0 mg (0.13 mmol) of **7a** to obtain 34.8 mg of **8a**, which consisted of white solid and mp. 291.3 °C–292.2 °C. **8a** was obtained in 47.6 % overall yield (2 steps from **6**). The ^{1}H-NMR (300 MHz, $CDCl_3$) conditions were as follows: 2.26 (s, 6 H), 5.73 (s, 1 H), 6.95 (bs, 1 H), 7.46 (td, 1 H, J = 7.6, 1.0 Hz), 7.56 (m, 2 H), 7.70 (s, 2 H), 7.74 (m, 1 H), 7.87 (m, 2 H), 7.91 (bd, 1 H, J = 8.6 Hz), 8.30 (dd, 1 H, J = 8.2, 1.1 Hz), and 9.96 (s, 1 H). The ^{13}C-NMR (75 MHz, $CDCl_3$) conditions were as follows: 16.1, 93.1, 104.0, 117.6, 118.2, 119.5, 121.5, 123.9, 127.3, 130.9, 132.5, 133.2, 134.1, 144.6, 148.7, 153.5, 155.2, 160.7, and 191.4. Finally, the HRMS (+ ESI) was $C_{25}H_{20}N_3O_2$ $[M + H]^+$; it requires 394.1550, but has 394.1559.

4-(2′,6′-Dimethyl-4′-cyanophenoxy)-2-(4′′-cyanophenyl)-aminoquinoline **(8b)**

With 60 % yield, the synthesis started with 70.0 mg (0.23 mmol) of **7b** to obtain 53.0 mg of **8b**, which consisted of white solid and mp. 256.5 °C–257.0 °C. **8b** was obtained in 37.2 % overall yield (2 steps from **6**). The ^{1}H-NMR (300 MHz, $CDCl_3$) conditions were as follows: 2.23 (s, 6 H), 5.81 (s, 1 H), 7.41–7.46 (m, 1 H), 7.47 (s, 2 H), 7.56 (dd, 2 H, J = 7.1, 1.8 Hz), 7.71 (m, 1 H), 7.87–7.99 (m, 3 H), and 8.27

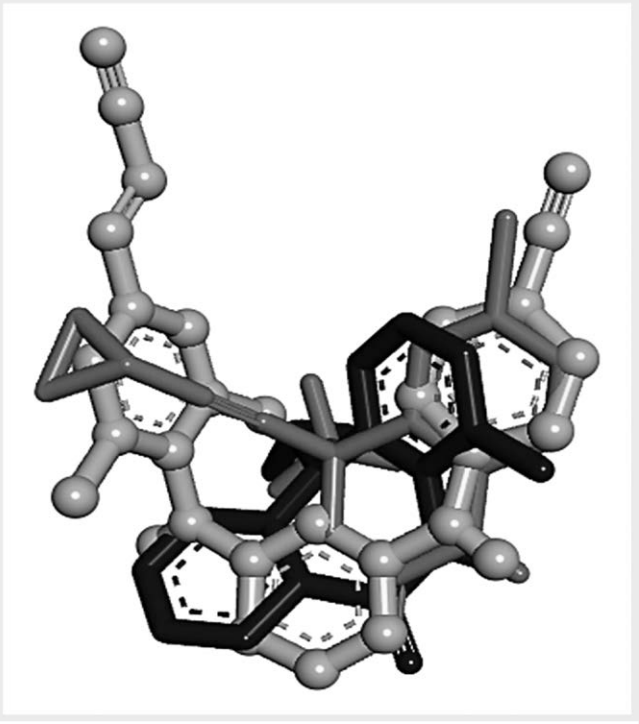

▶ **Fig. 1** Overlay of the conformations of nevirapine (NVP) (black), efavirenz (EFV) (dark grey), and rilpivirine (TMC278) (light grey) in the binding pocket of HIV-1 RT.

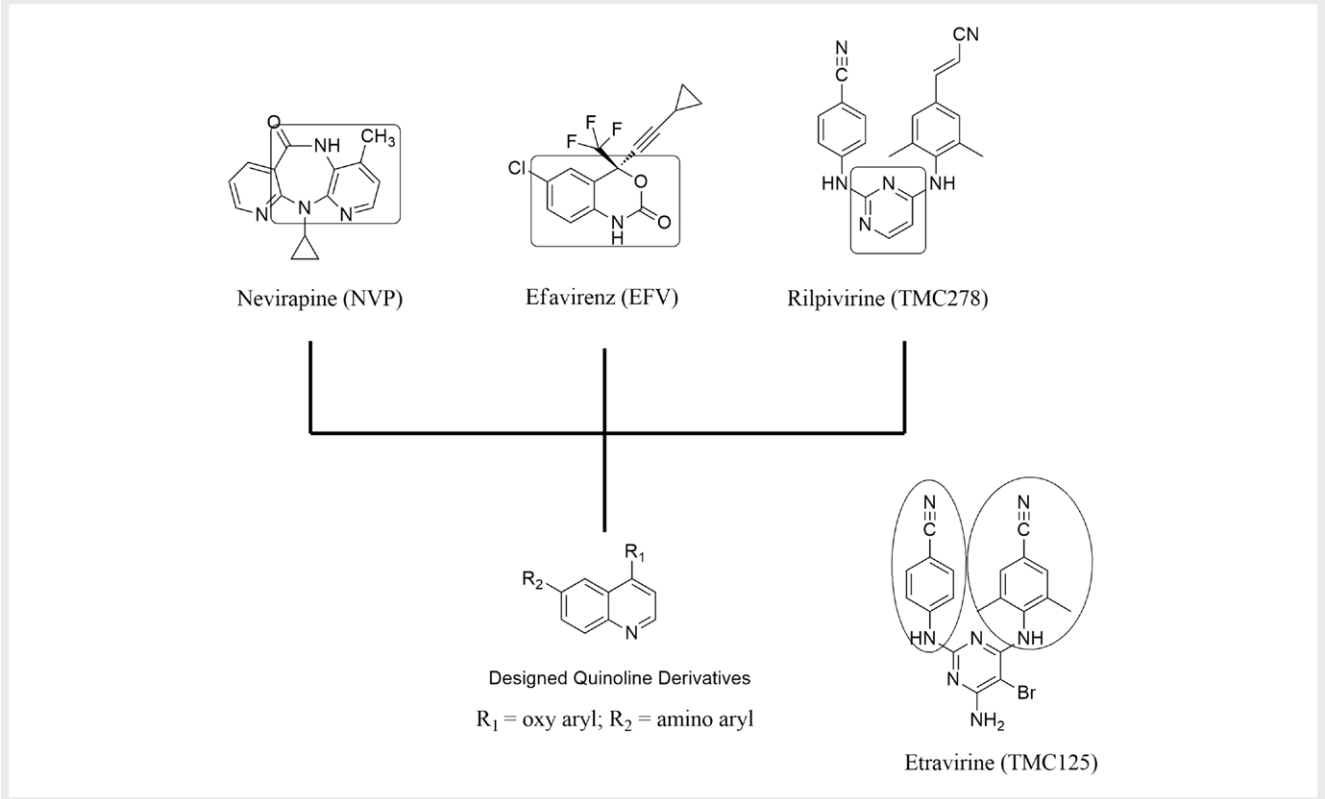

▶ **Fig. 2** Design of a disubstituted quinoline based on the structure guide using the molecular hybridization of NVP, EFV and TMC278 as the basic structure.

(dd, 1 H, J = 8.2, 1.1 Hz). The ^{13}C-NMR (75 MHz, $CDCl_3$) conditions were as follows: 16.0, 93.3, 103.6, 109.4, 117.4, 118.2, 119.6, 121.3, 123.8, 127.2, 130.9, 133.0, 133.1, 133.2, 144.8,148.6, 153.8, 154.0, and 160.2. Finally, the HRMS (+ ESI) was $C_{25}H_{19}N_4O$ $[M + H]^+$; it requires 391.1553, but has 391.1548.

4-(4′-formylphenoxy)-2-(4′′-cyanophenyl)-aminoquinoline **(8c)**

With 62 % yield, the synthesis started with 70.0 mg (0.25 mmol) of **7c** to obtain 55.9 mg of **8c**, which consisted of white solid and mp. 267.1 °C–268.0 °C. **8c** was obtained in 41.5 % overall yield (2 steps from **6**). The ^{1}H-NMR (300 MHz, $CDCl_3$) conditions were as follows: 6.42 (s, 1 H), 7.43 (t, 1 H, J = 7.1 Hz), 7.50–7.59 (m, 2 H), 7.66–7.77 (m, 3 H), 7.77–7.88 (m, 1 H), 8.04–8.15 (m, 4 H), 9.80 (s, 1 H), and 10.1 (s, 1 H). The ^{13}C-NMR (75 MHz, DMSO-d6) conditions were as follows: 97.8, 102.0, 117.6, 117.9, 119.6, 121.2, 123.6, 126.7, 130.7, 132.1, 133.1, 133.5, 145.4, 148.1, 154.1, 159.1, 160.4 and 191.9. Finally, the HRMS (+ ESI) was $C_{23}H_{16}N_3O_2$ $[M + H]^+$; it requires 366.1237, but has 366.1229.

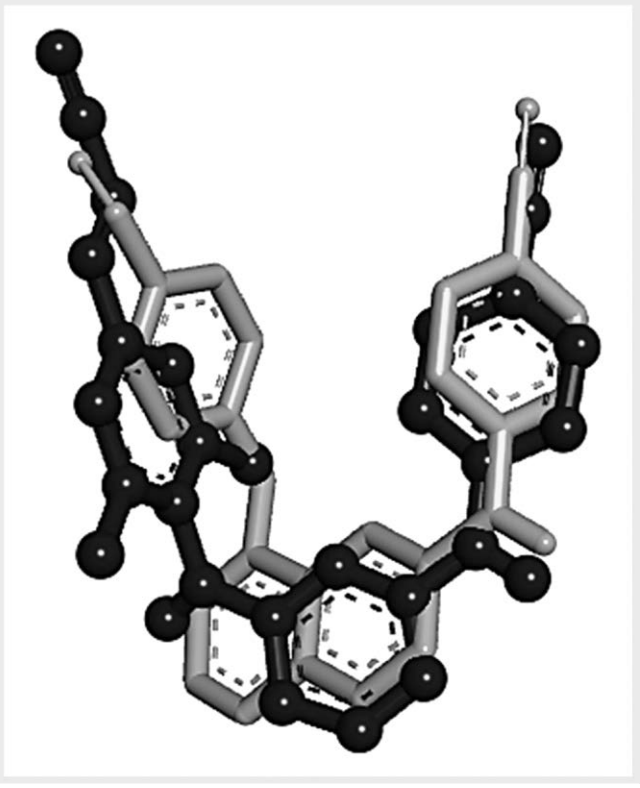

▶ **Fig. 3** Conformations of rilpivirine (TMC278) (black) and 4-(4′-formylphenoxy)-6-(4′′-cyanophenyl)-aminoquinoline (grey) in the binding pocket of HIV-1 RT.

4-(4′-cyanophenoxy)-2-(4′′-cyanophenyl)-aminoquinoline **(8d)**

With 59 % yield, the synthesis started with 70.0 mg (0.25 mmol) of **7d** to obtain 53.3 mg of **8d**, which consisted of white solid and mp. 278.5 °C–278.7 °C. **8d** was obtained in 35.4 % overall yield (2 steps from **6**). The ^{1}H-NMR (300 MHz, $CDCl_3$) conditions were as follows: 6.59 (s, 1 H), 7.18–7.24 (m, 2 H), 7.25–7.31 (m, 2 H), 7.47–7.54 (m, 1 H), 7.60–7.65 (m, 3 H), 7.66–7.80 (m, 3 H), and 8.08 (d, 1 H, J = 7.9 Hz). The ^{13}C-NMR (75 MHz, $CDCl_3$) conditions were as follows: 103.9, 108.5, 118.1, 119.8, 119.9, 121.6, 125.9, 126.9, 128.0, 131.1, 133.2, 134.4, 147.8, 148.7, 156.0, 158.7, and 160.2. Finally, the HRMS (+ ESI) was $C_{23}H_{15}N_4O$ $[M + H]^+$; it requires 363.1240, but has 363.1232.

HIV-1 RT inhibition assay

The inhibition assay of HIV-1 RT (wt) was performed by utilizing the template/primer hybrid poly(A) × oligo $(dT)_{15}$, digoxigenin- and biotin-labeled nucleotides, an antibody to digoxigenin that was conjugated to peroxidase (anti-DIG-POD), and the peroxidase substrate ABTS. The incorporation quantities of the digoxigenin- and biotin-labeled dUTP into DNA represented the activity of HIV-1 RT activity. The HIV-RT inhibition assay was implemented using an RT assay kit (Roche), and the procedures for assaying RT inhibition were performed as described in the kit protocol [18–20]. The tested compound and the three control drugs, namely, NVP, EFV, and TMC278, were used at 1 µM concentration to determine the percentage inhibitory values. The reaction mixture consisted of template/primer complex, 2′-deoxy-nucleotide-5′–triphosphates (dNTPs), and RT enzyme in the lysis buffer with or without an inhibitor. After incubation for 1 h at 37 °C, the reaction mixture was transferred to streptavidin-coated microtiter plate (MTP). The biotin-labeled dNTPs that were incorporated in the template because of the presence of RT were bound to strepavidine. The unbound dNTPs were washed using a wash buffer, and then, antidigoxigenin-peroxidase

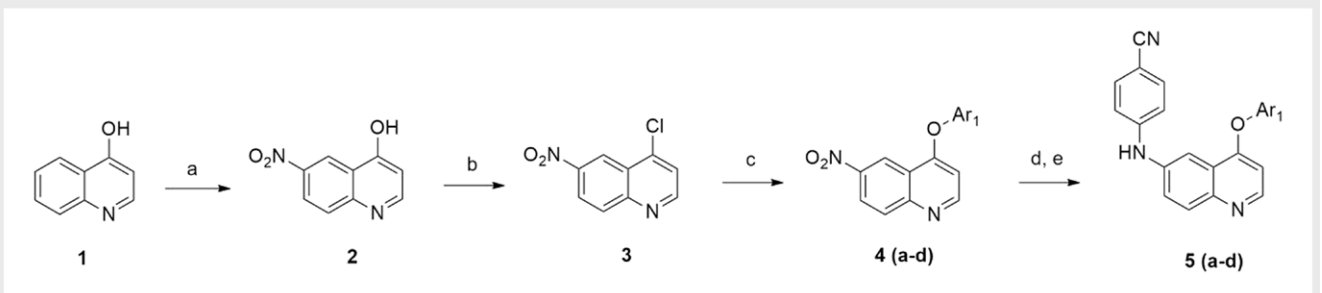

▶ **Fig. 4** Synthesis of 6-amino-4-oxydiaylquinoline derivatives Reagents and conditions: **a** HNO_3/H2SO_4, −15 °C to 0 °C; **b** $POCl_3$, cat. DMF, 100 °C sealed tube; **c** hydroxyl benzene (Ar_1OH), K_2CO_3, DMF, 100 °C sealed tube; **d** $SnCl_2$, EtOH, sonicated at 30 °C; **e** 4-iodobenzonitrile, $Pd(OAc)_2$, SPhos, Cs_2CO_3, DMF, 100 °C.

▶ **Table 1** Inhibitory activity (%) of the compounds **5(a-d)**, NVP, EFV, and TMC278 at 1 µM against HIV-1 RT.[a]

Compounds	Ar_1	inhibition (%) against HIV-1 RT[b]
5a	2,6-dimethyl-4-formylphenoxy	28.73 ± 2.01
5b	2,6-dimethyl-4-cyanophenoxy	25.46 ± 1.75
5c	4-formylphenoxy	34.91 ± 1.84
5d	4-cyanophenoxy	32.43 ± 1.50
NVP		53.39 ± 1.70
EFV		96.69 ± 0.85
TMC278		97.06 ± 0.98

[a]The RT kit was commercially available and supplied by Roche, and the data were obtained by standard ELISA. [b]Results were expressed as mean ± standard error of Inhibitory activity (%).

▶ **Table 2** The binding energy and the interaction between each of the 6-amino-4-oxydiarylquinoline derivatives **5(a-d)**, NVP, EFV and TMC278 and the HIV-1 RT from molecular docking.

Compound	Binding energy (kcal/mol)[a]	NOC[b]
5a	−12.01 ± 0.02	17 ± 3
5b	−12.16 ± 0.06	20 ± 5
5c	−11.80 ± 0.01	106 ± 6
5d	−12.21 ± 0.01	110 ± 3
NVP	−7.91 ± 0.01	125 ± 3
EFV	−9.25 ± 0.01	130 ± 5
TMC278	−12.53 ± 0.01	133 ± 5

[a]Results were expressed as mean ± standard error of binding energy (kcal/mol). [b]Results were expressed as mean ± standard error of number of ligand conformations

(anti-DIG-POD) was added to the MTP. The DIG-labeled dNTPs incorporated in the template was bound to the anti-DIG-POD antibody. The unbound anti-DIG-POD was also washed elaborately for 5 times by using a wash buffer. Finally, the peroxide substrate (ABST) was added to the MTP. A colored reaction product emerged during the cleavage of the substrate catalyzed by peroxide enzyme. The absorbance of the sample was measured at OD_{405} (reference wavelength: approx. 490 nm) by using the MTP (ELISA) reader. The percentage inhibitory activity of RT inhibitors was calculated by comparing with that of a sample without an inhibitor. The resulting color intensity was directly proportional to the RT activity. The percentage inhibitory values were calculated by the following formula: Inhibition % = {1−([O.D. value with RT and inhibitor−O.D. value without RT and inhibitors] / [O.D. value without inhibitors (with RT)−O.D. value without RT and inhibitors])} × 100.

Cytotoxic activity

Cell line were seeded in a 96-well microplate (Costar No. 3599), 100 µL/well, at a density of 5 × 10^3 to 2 × 10^4 cells/well. Background control wells contained the same volume as the complete culture medium. The microplate was incubated for 24 h at 37 °C, with 5 % CO_2, and 95 % humidity (Shellab). Samples at various concentrations were added to the microplate, which was incubated for another 48 h. Cell viability was determined by staining with the MTT assay [3(4,5-dimethylthiazol-2-yl)-2–5-diphenyl tetrazolium bromide (Sigma-Aldrich) [21–24]. The reagent was dissolved in phosphate buffered saline at 5 mg/mL, and filtered to sterilize and remove a small amount of insoluble residue present in some batches of MTT. MTT solution (10 µL/100 µL medium) was added to all wells of each assay, and plates were incubated at 37 ° C, 5 % CO_2, and 95 % humidity for 2–4 h. Subsequently, DMSO (100 µL, Merck, Germany) was added to dissolve the resulting formazan by sonication. The

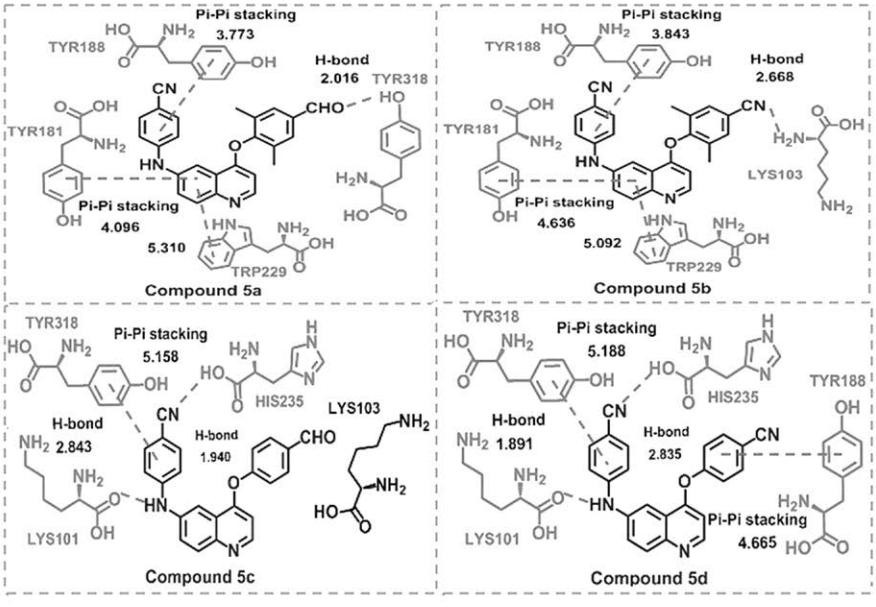

▶ **Fig. 5** Binding interactions between 6-amino-4-oxydiaylquinoline derivatives **5**(**a**-**d**) and HIV-1 RT surrounding the designed compounds (distance in °A).

plates were read on a microplate reader (Molecular Devices, CA, USA) by using a test wavelength of 550 nm and a reference wavelength of 650 nm. The XTT assay for suspension cells was acute lymphoblastic leukemia (MOLT-3) [23]. Plates were incubated for 4 h after the addition of 50 µL of mixture of 1 mg/mL (5 mL) and 0.383 mg/mL (100 µL) of phenazine methosulfate. The absorbance of the formed orange formazan compounds was measured at the wavelengths of 492 and 690 nm. IC_{50} values were determined as the drug and sample concentrations at 50 % inhibition of the cell growth.

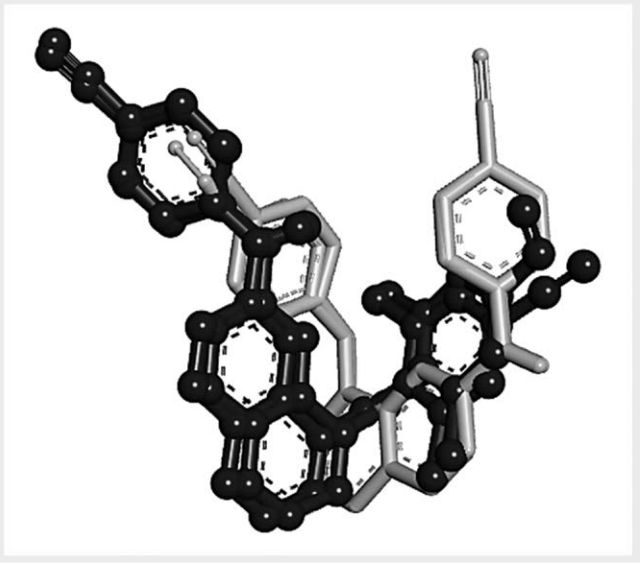

▶ **Fig. 6** Conformations of 6-amino-4-oxydiaylquinoline derivatives **5**(**a**-**b**) (black) and **5**(**c**-**d**) (grey) in the binding pocket of HIV-1 RT.

Results and Discussion

Molecular docking was used to predict the binding site, the binding energy and the interaction between assigned compounds and the HIV-1 RT to propose the potential of the assigned molecules in evaluating the new anti-HIV-1 RT agent. In our molecular docking approach, the new target molecule was obtained from the molecular hybridization for NVP, EFV and TMC278 with HIV-1 RT to observe the conformation and interaction between these compounds and the HIV-1 RT binding site. The combination and the overlaying of NVP, EFV and TMC278 in the binding site of HIV-1 RT allowed the development of a new hybrid structure, which was based on the subunits for each of the NVP, EFV, and TMC278, as shown in ▶ **Fig. 1**. Resulting from the molecular hybridization, 4,6-disubstituted quinoline was designed as a core structure that corresponded with the square frame as in ▶ **Fig. 2**. The 4,6-disubstituted quinoline may maintain the characteristics of the original base structure, especially in the EFV structure. The substituents in the assigned molecule were selected from those of TMC125 and TMC278 as an amino aryl and oxy aryl groups, respectively.

The molecular docking was applied to stimulate the conformations of the assigned molecules, that is, 4-(4'-formylphenoxy)-6-(4"-cyanophenyl)-aminoquinoline. The optimized molecule was arranged in a similar pattern with the TMC278 at the binding site of HIV-1 RT (▶ **Fig. 3**). Therefore, 6-amino-2-oxydiarylquinoline derivatives were selected and synthesized to observe the anti-RT activity.

6-Amino-4-oxydiarylquinoline **5(a-d)** was synthesized as shown in ▶ **Fig. 4**. The 6-nitroquinolin-4-ol **(2)** was obtained from the nitration of 4-hydroxy-6-nitroquinoline **(1)** using nitric and sulfuric acids. The 6-nitroquinolin-4-ol **(2)** was subjected with phosphorus oxychloride to afford the 4-chloro-6-nitroquinoline **(3)**. The 6-amino-4-oxydiarylquinoline **5(a-d)** was obtained from 4-chloro-6-nitroquinoline **(3)** by replacing the chlorine with hydroxyl benzene under basic conditions. 4-Oxyaryl-6-nitroquinoline **(4)** was treated with a reducing agent to generate aryl amine, followed by the cross

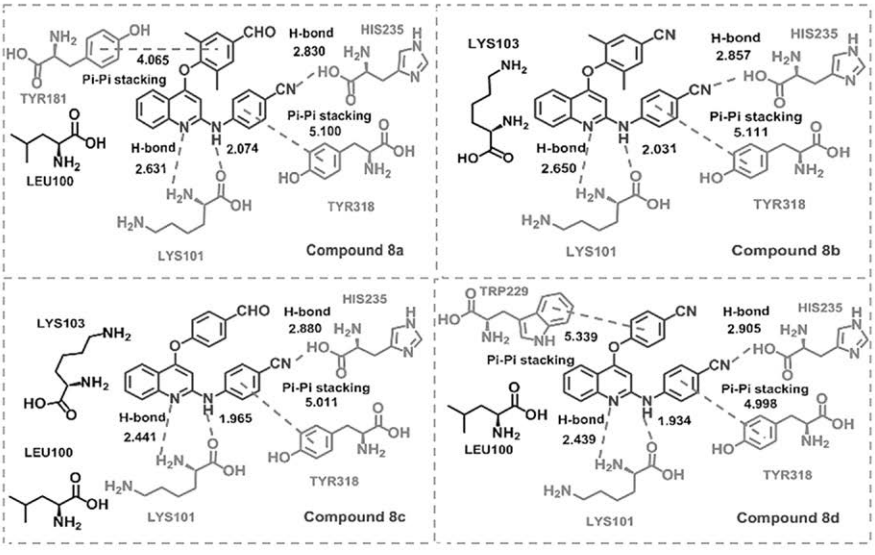

▶ **Fig. 7** Binding interactions between 2-amino-4-oxydiarylquinoline derivatives **8**(**a**-**d**) and HIV-1 RT surrounding the designed compounds (distance in °A).

coupling reaction with 4-iodobenzonitrile using $Pd(OAc)_2$ to obtain 6-amino-4-oxydiarylquinoline **5(a-d)**.

The 6-amino-4-oxydiarylquinoline derivatives **5(a-d)** were tested for percentage inhibitory activity against HIV-1 RT at 1 µM concentration for each of the synthesized compounds by using the RT assay and colorimetric method. The result was demonstrated in ▶ **Table 1**. The inhibitory activity (%) for each compound was lower than that of NVP, EFV, and TMC278, which were used as anti-RT drugs. The molecular docking was used to expand and support the experimental results; for instance, the anti-RT activity considered the designed molecules. The binding energy, the number of ligand conformation and the interaction for 6-amino-4-oxydiarylquinoline derivatives **5(a-d)** in the HIV-1 RT was calculated, as shown in ▶ **Table 2** and ▶ **Fig. 6**.

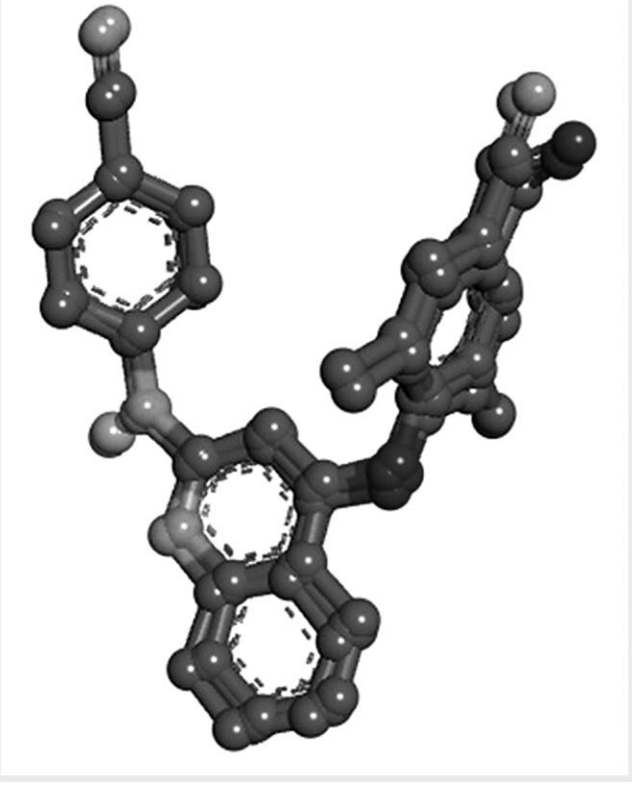

▶ **Fig. 8** Conformations of 2-amino-4-oxydiaylquinoline derivatives **8**(**a**-**d**) in the binding pocket of HIV-1 RT.

▶ **Table 3** Binding energy and the interaction between 2-amino-4-oxydiarylquinoline derivatives **8(a-d)** and HIV-1 RT from molecular docking.

Compound	Binding energy (kcal/mol)[a]	NOC[b]
8a	−13.18 ± 0.01	77 ± 8
8b	−13.69 ± 0.02	89 ± 6
8c	−12.06 ± 0.01	66 ± 4
8d	−12.56 ± 0.01	92 ± 4

[a]Results were expressed as mean ± standard error of binding energy (kcal/mol). [b]Results were expressed as mean ± standard error of number of ligand conformations

The binding energies of **5(a-d)** are relatively similar and lower than those of anti-RT drugs, thereby possibly causing a higher stability for the interaction. In the molecular docking, we found that **5(a-d)** were bound to the same location in the HIV-1 RT. From ▶ **Fig. 5**, the aromatic ring in the core structure and in the substituent at 6-position of quinoline **5(a-b)** exhibited the hydrophobic interactions with the indole ring of Trp229 and with the aromatic ring of Tyr188 and Tyr181 by using π-π stacking interaction in the HIV-1 RT. Moreover, the formyl group and the cyano group in the substituent at 4-position of quinoline **5(a, b)** displayed the hydrogen bond interactions with the hydroxyl group of Try318 and with the amino group of Lys103 in the HIV-1 RT, respectively. Whereas, the NH-amino group and the cyano group in the substituent at 6-position of quinoline **5(c-d)** demonstrated the hydrogen bonding interactions with the carboxyl group on Lys101 and with the carboxylic acid group on His235. The hydrogen bonding interaction between **5(c-d)** and HIV-1 RT displayed shorter, and greater than that of **5(a-b)**, moreover, the number of ligand conformation of **5(c-d)** exhibited five times of **5(a-b)**. Thus, the different conformations and interaction for each of the compounds had various effects on the anti-RT activity. Additionally, **5(c-d)** exhibited an anti-RT activity that was higher than that of **5(a-b)**, thereby corresponding to the interaction information from the molecular docking. According to many studies, the hydrogen bonding interaction between the active compounds and the Lys101 residue in the HIV-1 RT is often found in NNRTIs [25]. From those results, some compounds demonstrated different conformations and interaction, as shown in ▶ **Fig. 5** and **6**. The 6-amino-4-oxydiarylquinoline derivatives may not be suitable for the interaction and binding with HIV-1 RT because the conformations were not arranged in the same pattern, resulting in difficulty in studying and designing the target molecules. Therefore, 2-amino-4-oxydiarylquinoline derivatives **8(a-d)** were assigned and docked instead of the 6-amino-4-oxydiarylquinoline **5(a-d)** to observe the potent HIV-1 NNRTIs.

Molecular docking results of 2-amino-4-oxydiarylquinoline quinoline derivatives **8(a-d)** showed that all compounds bound to

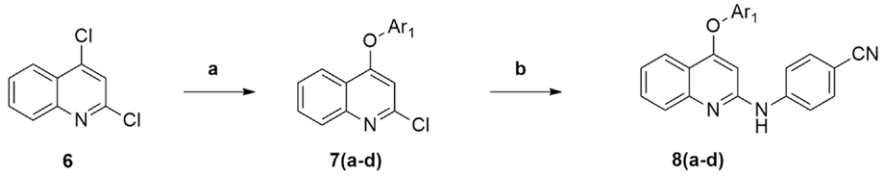

▶ **Fig. 9** Synthesis of 2-amino-4-oxydiaylquinoline derivatives Reagents and conditions: **a** hydroxyl benzene (Ar_1OH), Cs_2CO_3, DMF, 80 °C sealed tube; **b** 4-iodobenzonitrile, $Pd(OAc)_2$, SPhos, Cs_2CO_3, DMF, 100 °C.

HIV-1 RT with an identical location using 3 hydrogen bonding. First bonding structured from the nitrogen atom in the quinoline core-structure with the hydrogen atom of the amino group on Lys101. Second bonding created from the hydrogen atom in the amino substituent at 2-position of quinoline with the oxygen atom of the carboxyl group on Lys101. Third bonding displayed from the nitrogen atom in the cyano group at the side chain of substituent in 2-position of quinoline with the hydrogen atom of the carboxylic acid group on His235 as shown in ▶ **Fig. 7** and **8**. The aldehyde group on **8a** and **8c** and the cyano group on **8b** and **8d** indicated different binding energies, as demonstrated in ▶ **Table 3**. Comparing the substituent effect between the cyano group (**8c**) and the aldehyde group (**8d**) on the binding site with HIV-1 RT, we found that **8d**, which was the derivative with the cyano group, indicated considerably greater binding energy values than **8c**, which was the derivative with the aldehyde group. Meanwhile, the addition of methyl group to the aromatic cyano derivative (**8b**) led to an improved binding corresponded with the binding energy obtained from the addition of methyl group to the aromatic aldehyde derivative (**8a**). Thus, 2,4-disubstitued quinoline as 2-amino-4-oxydiarylquinoline derivatives **8(a-d)** may provide a stronger inhibiting activity for HIV-1 RT than 6-amino-4-oxydiarylquinoline derivatives **5(a-d)**.

The 2-amino-4-oxydiarylquinoline derivatives **8(a-d)** were synthesized from 2,4-dichloroquinoline (**6**) by using nucleophilic substitution reaction under basic conditions, followed by cross-coupling reaction as shown in the ▶ **Fig. 9**. The 2-amino-4-oxydiarylquinoline **8(a-d)** was subjected to testing the percentage inhibitory activity against HIV-1 RT, with the RT assay using the colorimetric method; the result is presented in ▶ **Table 4**.

The 2-amino-4-oxydiarylquinoline **8(a)** demonstrated a higher inhibitory activity against HIV-1 RT than **8(c)**. The result was corresponded with the information from the molecular docking and the interaction with the HIV-1 RT. The binding energy of **8(a)** was exhibited lower than **8(c)**, and, the NOC value of **8(a)** was showed higher than **8(c)**. Additionally, the hydrophobic interaction between the aromatic substituent at 4-position of quinoline and the aromatic ring of Tyr181 was found only in **8(a)**. Moreover, the 2-amino-4-oxydiarylquinoline **8(d)** exhibited a stronger inhibitory activity against HIV-1 RT than **8(b)**, thereby corresponding to the information from the interaction with the HIV-1 RT. **8(d)** displayed the hydrophobic interaction between the aromatic substituent at 4-position of quinoline and the indole ring of Trp229, whereas **8(b)** was not. The molecular docking results of 2-amino-4-oxydiarylquinoline derivatives **8(a-d)** showed that **8(d)** provided the best value of the number of ligand conformation. Those results implied that **8(d)** have a good inhibitory activity compared with other designed compounds. However, the activity may not be corresponded to the molecular docking in some cases, because the molecular docking was used to predict the binding side, binding energy, and the interaction between designed compounds and the receptors in the computer, thereby possibly causing a different result in the biological testing. Besides the inhibition of HIV-1 RT activity, 2-amino-4-oxydiaylquinoline derivatives **8(a-d)** and three common drugs (NVP, EFV, and TMC278) were evaluated for cytotoxicity against various cancer cell lines, as shown in ▶ **Table 5**. In the literatures, the NNRTIs, namely, NVP, EFV, and TMC278, have been reportedly toxic against a wide range of cancer cells in vitro [26–33] and only have been reported a minor toxicity against normal tissue cells [26]. The toxicity of NNRTIs against cancer cells promoted the idea to use these drugs in patients infected with HIV-1 to prevent or even treat cancer. In a cytotoxic assay, **8b**, **8d** and NVP demonstrated a weak activity against the evaluated cancer cell lines and normal cell lines (MRC-5). **8a**, **8c**, EFV, and TMC278 exhibited a strong activity against acute lymphoblastic leukemia (MOLT-3) cells (IC_{50} values

▶ **Table 4** Inhibitory activity (%) of the compounds **8(a-d)** against HIV-1 RT.[a]

Compounds	Ar_1	inhibition (%) against HIV-1 RT[b]
8a	2,6-dimethyl-4-formylphenoxy	34.02 ± 2.37
8b	2,6-dimethyl-4-cyanophenoxy	27.85 ± 1.64
8c	4-formylphenoxy	19.40 ± 1.62
8d	4-cyanophenoxy	39.71 ± 1.67

[a]The RT kit was commercially available and supplied by Roche, and data were obtained by standard ELISA. [b]Results were expressed as mean ± standard error of Inhibitory activity (%).

▶ **Table 5** In vitro cytotoxic activity of the compounds **8(a-d)** against human cancer cell lines and normal cell line.

Compounds	Cell lines[a] [IC_{50} (μg/mL)][b]				
	HepG2	MOLT-3	HuCCA-1	A549	MRC-5
8a	25.95 ± 2.40	4.63 ± 0.62	11.58 ± 0.768	20.13 ± 1.195	27.46 ± 1.68
8b	%C = 38.25[c]	19.04 ± 16.02	%C = 3.00[c]	%C = 21.00[c]	%C = 7.36[c]
8c	26.76 ± 2.80	5.71 ± 1.33	10.84 ± 0.735	44.46 ± 1.647	39.41 ± 1.73
8d	%C = 44.80[c]	%C = 6.00[c]	%C = 23.00[c]	%C = 26.00[c]	%C = 12.03[c]
NVP	%C = 15.37[c]	%C = 29.00[c]	%C = 11.00[c]	%C = 18.00[c]	%C = 1.02[c]
EFV	27.33 ± 1.23	7.76 ± 0.37	18.83 ± 0.756	19.00 ± 0.565	30.17 ± 1.90
TMC278	32.02 ± 4.19	1.57 ± 0.20	22.46 ± 0.621	%C = 42.00[c]	%C = 14.42[c]
Doxorubicin	0.23 ± 0.02	–	0.89 ± 0.035	0.19 ± 0.007	1.42 ± 0.04
Etoposide	21.14 ± 0.70	0.048 ± 0.007	–	–	–

[a]HepG2 (Hepatocarcinoma), MOLT-3 (Acute lymphoblastic leukemia), HuCCA-1 (Cholangiocarcinoma), A549 (Lung carcinoma), MRC-5 (normal embryonic lung cell). [b]Results were expressed as mean ± standard error of inhibition perceptual for all cell lines. Doxorubicin and etoposide were used as the positive control. Experiments were performed in triplicate. [c]Inactive (IC_{50} ≥ 50 μg/mL); reported in percentage cytotoxicity at the substance concentration of 50 μg/mL.

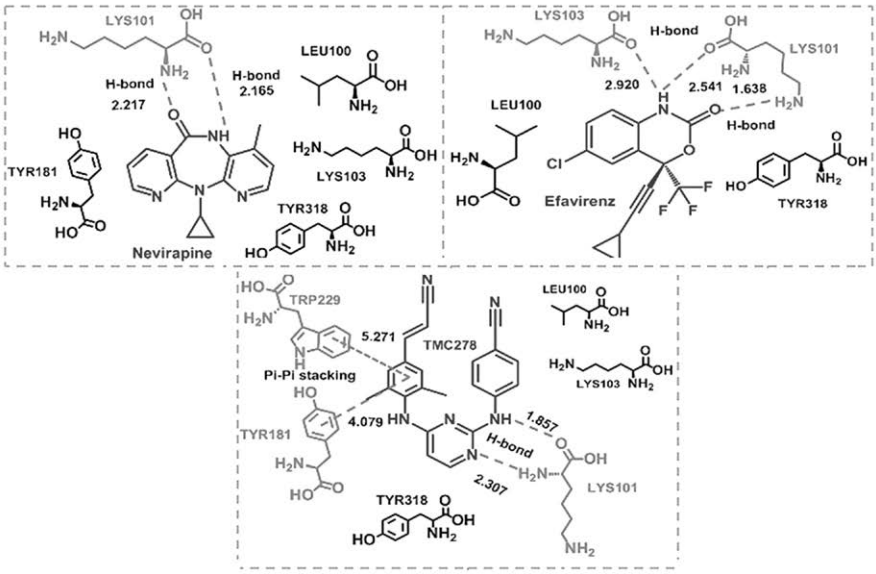

▶ **Fig. 10** Binding interactions between nevirapine (NVP), efavirenz (EFV), and rilpivirine (TMC278) and HIV-1 RT surrounding the designed compounds (distance in °A).

of 4.63 ± 0.62, 5.71 ± 1.33, 7.76 ± 0.37 and 1.57 ± 0.20 µg/mL, respectively). **8a**, **8c**, EFV, and TMC278 had substantial cytotoxicity in the evaluated cancer cell line whereas TMC278 had moderate cytotoxicity against normal embryonic lung (MRC-5) cells. However, **8d** had high percentage inhibitory activity against HIV-1 RT compared with other synthesized compounds and had very low cytotoxic against normal embryonic lung (MRC-5) cells compared with EFV and TMC278.

Finally, in this study, we also reported the binding energies, number of conformations, interactions and characterization of new HIV-1 RT inhibitors that evaluated the possibility to use quinoline as a structure basis. The molecular docking results of efavirenz, nevirapine and rilpivirine demonstrated that all compounds bound to HIV-1 RT on Lys101 using hydrogen bonding except for the efavirenz, that also bound on Lys103 using hydrogen bonding. π-π stacking between HIV-1 RT in the amino acid residue named of Trp229 and Tyr181 and rilpivirine were also found in the interaction information from the molecular docking calculation, as shown in ▶ **Fig. 10**. The interactions between rilpivirine or the designed compound **8a** and **8d** and HIV-1 RT were similar to those of hydrogen bonding and π-π stacking, with similar distance for each of amino acid residue. However, **8a** and **8d** exhibited more hydrogen bonding interaction which was displayed between His235, amino acid residue in HIV-1 RT, with the cyano group, side chain of substituent in 2-position of quinoline. Compound **8a** and **8d** have possessed percentage inhibitory against HIV-1 RT at 34.0 and 39.7 %, respectively. Those values are less than that of the commercial drugs which was used for the molecular hybridization such as NVP, EFV and TMC278. Based on the structure of **8a**, we found that adding the nitrogen atom into the quinoline core-structure such as 1,6-naphthyridine, together with the aromatic substituent at 2-position of quinoline demonstrated high NOC value and low biding energy. It means that the physicochemical properties and the pharmacological properties of 2-amino-4-oxydiarylquinoline derivatives may be improved using the Lewis base as nitrogen atom to increase the interaction such as the number of hydrogen bonding resulting to strong binding and good solubility. Further improve the structure and the activity for HIV-1 RT inhibitor and also the efficiency synthetic method of these 2-amino-4-oxydiarylquinoline derivatives are underway in our laboratory and will be reported in the near future.

Conclusions

2-amino-4-oxydiarylquinoline derivatives could inhibit HIV-1 RT at a stronger manner than 6-amino-4-oxydiarylquinoline, except for the 4-formylphenoxy substituent. According to the molecular docking results, the 2-amino-4-oxydiarylquinoline was more suitable for binding with the HIV-1 RT and more possible to study the substituent effect than the 6-amino-4-oxydiarylquinoline, because the former bound with the HIV-1 RT with an identical location. The percentage inhibitory activity against HIV-1 RT was also influenced by the substituent in the aromatic side chain of oxy-amino-aryl-quinoline. Furthermore, 4-(2′,6′-Dimethyl-4′-formylphenoxy)-2-(4′′-cyanophenyl)-aminoquinoline (**8a**) and 4-(4′-cyanophenoxy)-2-(4′′-cyanophenyl)-aminoquinoline **(8d)** could inhibit HIV-1 RT at the level similar with that of NVP. In addition, **8a** exhibited a strong cytotoxic activity against MOLT-3 cells, similar with those of EFV and TMC278. **8d** demonstrated very low cytotoxicity against normal embryonic lung (MRC-5) cells. Therefore, 2-amino-4-oxydiarylquinoline derivatives can be further improved for the development of HIV-1 RT inhibitors, thereby providing the opportunity to treat HIV and cancer with one drug.

Acknowledgements

The authors are grateful for the financial support given by Chulabhorn Research Institute during this study.

Conflict of Interest

The authors have declared no conflict of interest.

References

[1] Mathes T, Pieper D, Antoine SL et al. Adherence-enhancing interventions for highly active antiretroviral therapy in HIV-infected patients–A systematic review. Hiv Med 2013; 14: 583–595

[2] Slama L, Xiuhong Li, Brown T et al. Increases in duration of first highly active antiretroviral therapy over time (1996–2009) and associated factors in the multicenter AIDS cohort study. J Acquir Immune Defic Syndr 2014; 65: 57–64

[3] Ashchop EL, Wainberg MA, Sloan RD et al. Antiviral drug resistance and the need for development of new HIV-1 reverse transcriptase inhibitors. Antimicrob Agents Chemother 2012; 56: 5000–5008

[4] Vivet-Boudou V, Didierjean J, Isel C et al. Nucleoside and nucleotide inhibitors of HIV-1 replication. Cell Mol Life Sci 2006; 63: 163–186

[5] Pedersen OS, Pederson EB. Non-nucleoside reverse transcriptase inhibitors: The NNRTI boom. Antiviral Chem Chemother 1999; 10: 285–314

[6] de Bethune MP. Non-nucleoside reverse transcriptase inhibitors (NNRTIs), their discovery, development, and use in the treatment of HIV-1 infection: A review of the last 20 years (1989-2009). Antiviral Res 2010; 85: 75–90

[7] Sluis-Cremer N, Tachedjian G. Mechanisms of inhibition of HIV replication by non-nucleside reverse transcriptase inhibitors. Virus Res 2008; 134: 147–156

[8] Domaoal RA, Demeter LM. Structural and biochemical effects of human immunodeficiency virus mutants resistant to non-nucleoside reverse transcriptase inhibitors. Int J Biochem Cell Biol 2004; 36: 1735–1751

[9] Mehellou Y, De Clercq E. Twenty-Six Years of anti-hiv drug discovery: Where do we stand and where do we go? J Med Chem 2010; 53: 521–538

[10] Ludovici DW, De Corte BL, Kukla MJ et al. Evolution of anti-HIV drug candidates. Part 3: Diarylpyrimidine (DAPY) analogues. Bioorg Med Chem Lett 2001; 11: 2235–2239

[11] Jannen PA, Lewi PJ, Arnold E et al. In Search of a novel anti-HIV drug: Multidisciplinary coordination in the discovery of 4-[[4-[[4-[(1E)-2-Cyanoethenyl]-2,6-dimethylphenyl]amino]-2- pyrimidinyl]amino] benzonitrile (R278474, Rilpivirine). J Med Chem 2005; 48: 1901–1909

[12] Kumar S, Bawa S, Gupta H. Biological activities of quinoline derivatives. Mini-Rev Med Chem 2009; 9: 1648–1654

[13] Acharya BN, Thavaselvam D, Kaushik MP. Synthesis and antimalarial evaluation of novel pyridine quinoline hybrids. Med Chem Res 2008; 17: 487–494

[14] Assefa H, Kamath S, Buolamwini JK. 3D-QSAR and docking studies on 4-anilinoquinazoline and 4-anilinoquinoline epidermal growth factor receptor (EGFR) tyrosine kinase inhibitors. J Comput Aided Mol Des 2003; 17: 475–493

[15] Baba A, Kawamura N, Makino H et al. Studies on disease-modifying antirheumatic drugs: Synthesis of novel quinoline and quinazoline derivatives and their anti-inflammatory effect. J Med Chem 1996; 39: 5176–5182

[16] Fernandez-Bachiller MI, Perez C, Gonzalez-Munoz GC et al. Novel tacrine–8-hydroxyquinoline hybrids as multifunctional agents for the treatment of Alzheimer's disease, with neuroprotective, cholinergic, antioxidant, and copper complexing properties. J Med Chem 2010; 53: 4927–4937

[17] Jain S, Chandra V, Jain PK et al. Comprehensive review on current developments of quinoline-based anticancer agents. Arab J Chem 2016 In press

[18] Ukkonen P, Korpela J, Suni J et al. Inactivation of human immunodeficiency virus in serum specimens as a safety measure for diagnostic immunoassays. Eur J Clin Microbiol & Infect Dis 1988; 7: 518–523

[19] Reverse Transcriptase Assay. Colorimetric kit, Roche Diagnostics GmbH, Roche, Applied Science, Sandhofer Strasse. 116: D-68305 Mannheim, Germany:

[20] Suzuki K, Craddock BP, Okamoto N et al. Poly A-linked colorimetric microtiter plate assay for HIV reverse transcriptase. J Virol Methods 1993; 44: 189–198

[21] Mosman T. Rapid colorimetric assay for cellular growth and survival: Application to proliferation and cytotoxicity assays. J Immunol Methods 1983; 65: 55–63

[22] Carmichael J, Degraff WG, Gazdar AF et al. Evaluation of a tetrazolium-based semi-automated colormetric assay: Assessment of chemosensitivity testing. Cancer Res 1987; 47: 936–942

[23] Doyly A, Griffiths JB. Eds. Mammalian Cell Culture-essential Techniques. Chichester: Wiley & Sons; 1997

[24] Tominaga MH, Ishiyama M, Ohseto F et al. A water-soluble tetrazolium salt useful for colorimetric cell viability assay. Anal Commun 1999; 36: 47–50

[25] Ren J, Nichols CE, Stamp A et al. Structure insights into mechanisms of non-nucleoside drug resistance for HIV-1 reverse transcriptases mutated at codons 101 or 138. FEBS Journal 2006; 273: 3850–3860

[26] Hecht M, Harrer T, Buttner M et al. Cytotoxic effect of efavirenz is selective against cancer cells and associated with the cannabinoid system. AIDS 2013; 27: 2031–2040

[27] Sciamanna I, Landriscina M, Pittoggi C et al. Inhibition of endogenous reverse transcriptase antagonizes human tumor growth. Oncogene 2005; 24: 3923–3931

[28] Landriscina M, Fabiano A, Altamura S et al. Reverse transcriptase inhibitors down-rehulate cell proliferation in vitro and in vivo and restore thyrotropin signaling and iodine uptake in human thyroid anaplastic carcinoma. J Clin Endocrinol Metab 2005; 90: 5663–5671

[29] Mangiacasale R, Pittoggi C, Sciamanna I et al. Exposure of normal and transformed cells to nevirapine, a reverse transcriptase inhibitor, reduces cell growth and promotes differentiation. Oncogene 2003; 22: 2750–2761

[30] Pittoggi C, Martis G, Mastrangeli G et al. In vitro evidence for a new therapeutic approach in renal carcinoma. Int Braz J Urol 2008; 34: 492–502

[31] Sciamanna I, Gualtieri A, Cossetti C et al. A tumor-promoting mechanism mediated by retrotransposon-encoded reverse transcriptase is active in human transformed cell lines. Oncotarget 2013; 4: 2271–2287

[32] Sinibaldi-Vallebona P, Lavia P, Garaci E et al. A role for endogenous reverse transcriptase in tumorigenesis and as a target in differentiating cancer therapy. Genes Chromosomes Cancer 2006; 45: 1–10

[33] Stefanidis K, Loutradis D, Vassiliou LV et al. Nevirapine induces growth arrest and premature senescence in human cervical carcinoma cells. Gynecologic oncology 2008; 111: 344–349